The Radio Sky

Lecture 16

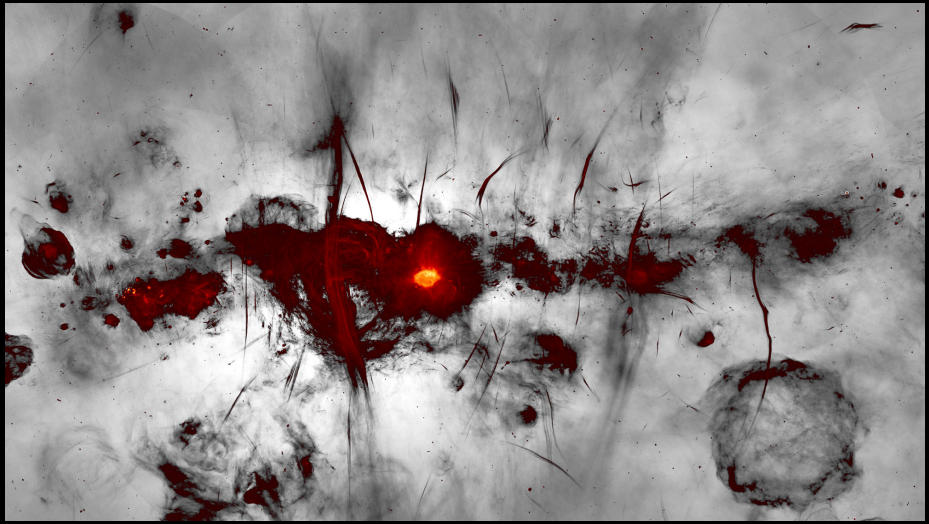
Yogesh Wadadekar

National Centre for Radio Astrophysics (NCRA-TIFR), Pune

PHY-236.3



The Galactic Centre at 1.28 GHz with MeerKAT



Credit: MeerKAT 1.28 GHz mosaic; plausibly SARAO / Heywood et al. 2022, doi:10.3847/1538-4357/ac449a.
Image index source: "Spitzer | HST | SDSS" [attribution to be confirmed]

Reading the mosaic

- 20 pointings, 144 h, 6.5 deg^2, $4''$ resolution (Heywood et al. 2022).
- Bright centre: the Sgr A complex.
- Long, thin vertical streaks: non-thermal filaments (NTFs); the brightest bundle is the Radio Arc.
- Clumpy emission along the plane: H II regions and star-forming complexes (Sgr B, Sgr C).
- Round shells: supernova remnants.
- Faint edges above and below the plane: the bipolar bubbles (Heywood et al. 2019).

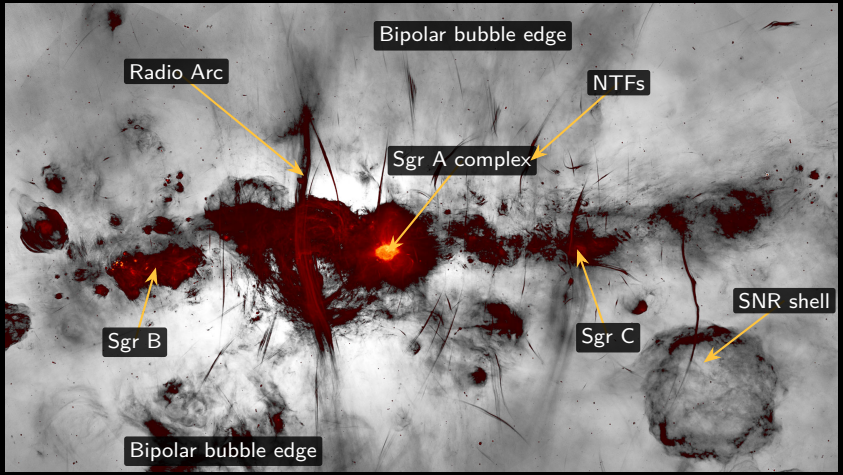
What the image alone gives

Observed: I_ν at 1.28 GHz, morphology, in-band α.

Not given: depth, physical association, density, B.

Inner $\sim 200\,\mathrm{pc}$: SMBH, star-formation rate and cosmic-ray energy densities $\sim 10^2\times$ the disc values (Heywood et al. 2022).

The mosaic annotated



Credit: MeerKAT 1.28 GHz mosaic; plausibly SARAO / Heywood et al. 2022, doi:10.3847/1538-4357/ac449a.
Labels added; positions approximate [attribution to be confirmed]

The radio components of the inner few hundred parsecs

Component	Size	Emission	First diagnostic
Sgr A*	$\lesssim$ AU	compact, flat/inverted	$T_{\rm b}$, VLBI size, variability
Sgr A West	$\sim 3\,\mathrm{pc}$	thermal free-free	$\alpha \approx -0.1$, RRLs
Sgr A East	$\sim 10\,\mathrm{pc}$ shell	synchrotron	steep α, polarization
CND	1.5–7 pc ring	molecular lines	NH_3, OH absorption
Radio Arc / NTFs	tens of pc long	synchrotron	polarization, α
Arches / Sickle	few pc	thermal free-free	RRLs, IR clusters
Sgr B2	$\sim$10 pc	H II + molecules	masers, NH_3, many lines
Bipolar bubbles	$\sim$430 pc	synchrotron edges	morphology, X-ray

Review: Morris & Serabyn 1996, doi:10.1146/annurev.astro.34.1.645. Sizes are approximate.

Free-free absorption gives depth order

Optically thin estimate from Lecture 4 (empirical approximation, ERA Ch. 4):

$$\tau_{\rm ff} \approx 3.28 \times 10^{-7} \left(\frac{T_{\rm e}}{10^4\,{\rm K}}\right)^{-1.35} \left(\frac{\nu}{\rm GHz}\right)^{-2.1} \left(\frac{\rm EM}{\rm pc\,cm^{-6}}\right)$$

EM (pc cm^{-6})	τ(0.33 GHz)	τ(1.4 GHz)
10^5	0.54	0.03
10^6	5.4	0.26
10^7	54	2.6

$T_{\rm e} = 7000$ K; illustrative EM values.

- At 330 MHz, Sgr A West appears in absorption against the non-thermal Sgr A East shell.
- Absorption requires the absorber to be in front: Sgr A West lies on the near side of Sgr A East (Pedlar et al. 1989, doi:10.1086/167635).

General tool: emission adds regardless of order; absorption needs a background source. It is one of the few depth diagnostics in an image.

Sgr A*: what is observed and what is inferred

Observed

- Compact, ∼Jy-level source with a flat to inverted cm spectrum ($\alpha \gtrsim 0$) rising to a sub-mm peak.
- Variable: hours (mm) to months (cm).
- Image size scaling as λ^2 at cm wavelengths.
- Stellar orbits (near-IR) and a ring at 1.3 mm.

Inferred

- Mass $\approx 4.15 \times 10^6\, M_\odot$ from stellar orbits (GRAVITY 2019; review: Genzel et al. 2010, doi:10.1103/RevModPhys.82.3121).
- Self-absorbed synchrotron from a low-luminosity accretion flow/jet: inverted spectrum, $T_\mathrm{b} \sim 10^{10}\,\mathrm{K}$.
- Scattering sets the cm image size.

Illustrative check

$S_\nu \approx 2.4\,\mathrm{Jy}$ at 230 GHz from a Gaussian of FWHM 52 μas gives $T_\mathrm{b} \approx 2 \times 10^{10}\,\mathrm{K}$. This needs electrons with $k_\mathrm{B} T \gtrsim m_\mathrm{e} c^2$: synchrotron from relativistic (possibly Maxwellian) electrons, not free-free from ordinary plasma.

How large should the black hole look?

Schwarzschild radius (exact for a non-rotating hole):

$$R_{\mathrm{S}} = \frac{2GM}{c^2} = \frac{2(6.67\times10^{-11})(4.15\times10^{6}\times1.99\times10^{30})}{(3.0\times10^{8})^2} = 1.2\times10^{10}\,\mathrm{m} \approx 0.08\,\mathrm{AU}.$$

The photon-capture ("shadow") diameter for a non-rotating hole is $2\sqrt{27}\,GM/c^2 \approx 5.2\,R_{\mathrm{S}}$ (spin changes it by $\lesssim 4\%$):

$$\theta_{\mathrm{sh}} = \frac{2\sqrt{27}\,GM}{c^2 R_0} \approx 52\,\mu\mathrm{as} \qquad (M = 4.15\times10^{6} M_{\odot},\ R_0 = 8.18\,\mathrm{kpc})$$

How large should the black hole look?

Schwarzschild radius (exact for a non-rotating hole):

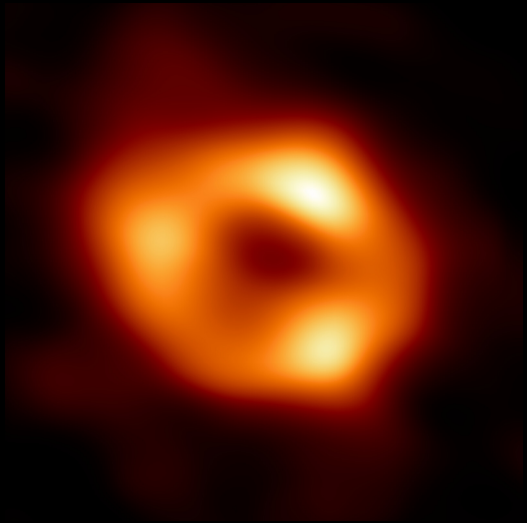
$$R_{\rm S} = \frac{2GM}{c^2} = \frac{2(6.67\times10^{-11})(4.15\times10^{6}\times1.99\times10^{30})}{(3.0\times10^{8})^2} = 1.2\times10^{10}\,\mathrm{m} \approx 0.08\,\mathrm{AU}.$$

The photon-capture ("shadow") diameter for a non-rotating hole is $2\sqrt{27}\,GM/c^2 \approx 5.2\,R_{\rm S}$ (spin changes it by $\lesssim 4\%$):

$$\theta_{\rm sh} = \frac{2\sqrt{27}\,GM}{c^2 R_0} \approx 52\,\mu\mathrm{as} \qquad (M = 4.15\times10^{6}M_\odot,\ R_0 = 8.18\,\mathrm{kpc})$$

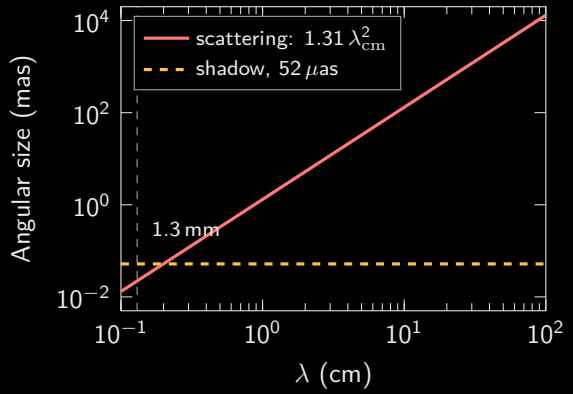
- EHT measured a ring of diameter $51.8 \pm 2.3\,\mu$as at 1.3 mm (EHT Collaboration 2022, doi:10.3847/2041-8213/ac6674).
- The ring diameter traces emission lensed near the photon ring: its relation to $\theta_{\rm sh}$ is calibrated with simulations, a model-dependent step.

Sgr A* at 1.3 mm with the Event Horizon Telescope



Credit: EHT Collaboration / ESO, CC BY 4.0, eso.org/public/images/eso2208-eht-mwa

Why the EHT observes at 1.3 mm: interstellar scattering



- Empirical fit to the major axis (Bower et al. 2006, doi:10.1086/508019): $\theta_{\rm scat} \approx 1.31\,{\rm mas}\,(\lambda/{\rm cm})^2$.
- At 20 cm: $\approx 0.5''$. At 1.3 mm: $\approx 22\,\mu$as, below the shadow size.
- λ^2 scaling is the signature of plasma scattering (Lecture 17).
- Intrinsic size needs the scattering kernel removed (Johnson et al. 2018, doi:10.3847/1538-4357/aadcff).

Concept test

Question

A compact Galactic-Centre feature is bright in synchrotron continuum but has no associated molecular-line emission (e.g. NH_3) at its position. Does that alone prove it is unrelated to molecular gas?

Concept test

Question

A compact Galactic-Centre feature is bright in synchrotron continuum but has no associated molecular-line emission (e.g. NH_3) at its position. Does that alone prove it is unrelated to molecular gas?

Answer: No

1. Projected line-of-sight structures can be unrelated, or physically associated but offset in depth or velocity.
2. A line non-detection also depends on excitation, optical depth, sensitivity, and interferometric filtering of extended emission.

Non-thermal filaments and the Radio Arc

- Discovered as the Radio Arc: parallel strands $\sim 0.25^\circ \approx 35\,\mathrm{pc}$ long, perpendicular to the plane (Yusef-Zadeh, Morris & Chance 1984, doi:10.1038/310557a0).
- MeerKAT: an order of magnitude more filaments; mean $\alpha \approx -0.83$, steeper than SNRs (-0.62), with large scatter (Yusef-Zadeh et al. 2022, doi:10.3847/2041-8213/ac4802).
- Strong linear polarization; B along the filaments.
- Equipartition $B \sim 100$–$400\,\mu$G (depends on the assumed proton/electron ratio).

Observed versus inferred

Observed: length, width, α, polarization angle and fraction.

Inferred: B (equipartition), electron energy, age, and origin. Origin of NTFs remains an open question.

Worked example: electrons in a filament

Assume $B = 100\,\mu\mathrm{G}$ (illustrative, from equipartition) and observe at $\nu = 1.28\,\mathrm{GHz}$. Single-particle results from Lecture 4 (SI). Characteristic frequency (pitch-angle factors of order unity dropped):

$$\nu_\mathrm{c} \approx 4.2\,\mathrm{MHz}\left(\frac{B}{\mathrm{G}}\right)\gamma^2 \;\Rightarrow\; \gamma \approx \left(\frac{1.28\times10^{9}}{4.2\times10^{6}\times10^{-4}}\right)^{1/2} \approx 1.7\times10^{3}$$

Loss time, with $U_B = B^2/2\mu_0$:

$$t_\mathrm{sync} = \frac{\gamma m_\mathrm{e} c^2}{\frac{4}{3}\sigma_\mathrm{T} c\,\gamma^2 U_B} \approx 1.4\,\mathrm{Myr}$$

Worked example: electrons in a filament

Assume $B = 100\,\mu\mathrm{G}$ (illustrative, from equipartition) and observe at $\nu = 1.28\,\mathrm{GHz}$. Single-particle results from Lecture 4 (SI). Characteristic frequency (pitch-angle factors of order unity dropped):

$$\nu_\mathrm{c} \approx 4.2\,\mathrm{MHz}\left(\frac{B}{\mathrm{G}}\right)\gamma^2 \;\Rightarrow\; \gamma \approx \left(\frac{1.28\times10^{9}}{4.2\times10^{6}\times10^{-4}}\right)^{1/2} \approx 1.7\times10^{3}$$

Loss time, with $U_B = B^2/2\mu_0$:

$$t_\mathrm{sync} = \frac{\gamma m_\mathrm{e} c^2}{\frac{4}{3}\sigma_\mathrm{T} c\,\gamma^2 U_B} \approx 1.4\,\mathrm{Myr}$$

- $E \approx 0.9\,\mathrm{GeV}$ electrons. Light travels $\sim 4\times10^{5}\,\mathrm{pc}$ in 1.4 Myr, so loss time does not limit a 35 pc filament; transport speed (Alfvén or diffusion) does.
- Steepening of α with distance from the plane is one proposed signature of ageing (Lecture 7).
- Every number here inherits the equipartition assumption.

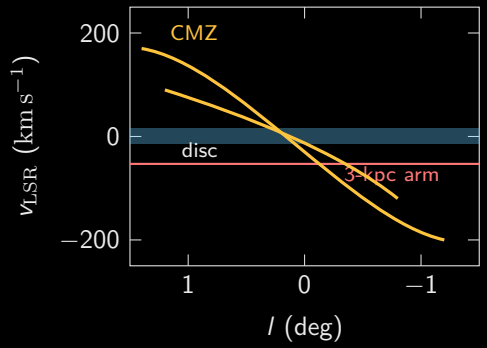
Velocity confusion along $l \approx 0$

For gas on circular orbits with angular speed $\omega(R)$, Galactocentric radius R, and Sun at R_0 (standard result, flat disc):

$$v_{\mathrm{LSR}} = R_0 \sin l \, [\omega(R) - \omega_0]$$

- At $l = 0$: $v_{\mathrm{LSR}} = 0$ for *all* circular-orbit gas, whatever its distance.
- Kinematic distances fail; foreground disc gas piles up near $0\,\mathrm{km\,s^{-1}}$.
- Departures from circular motion are then the signal: the 3-kpc arm absorbs at $\approx -53\,\mathrm{km\,s^{-1}}$; CMZ gas reaches $|v| \sim 200\,\mathrm{km\,s^{-1}}$ on non-circular (x_2/bar) orbits.

Schematic l–v diagram



H I and ionized gas: velocity confusion in practice

- H I absorption against Sgr A and other bright continuum sources: each absorption velocity is gas in front. Absorption at $-53\,\mathrm{km\,s^{-1}}$ places the 3-kpc arm in front of Sgr A.
- H I emission at $|v| \lesssim 20\,\mathrm{km\,s^{-1}}$ is dominated by the entire disc column: it is not a CMZ tracer.
- RRLs separate H II regions by velocity, but foreground diffuse ionized gas contributes low-velocity, broad, weak lines.
- Free-free continuum has no velocity at all: thermal emission from the disc and from the CMZ add in projection.

Rule

Association needs *matched velocities* in at least two tracers *and* a physical link. Overlap in (l, b) alone is not evidence.

Case study: the Galactic Centre magnetar

- PSR J1745−2900: a radio magnetar 2.4″ ($\approx 0.1\,\mathrm{pc}$ in projection) from Sgr A*.
- $\mathrm{DM} \approx 1778\,\mathrm{pc\,cm^{-3}}$ and $\mathrm{RM} \approx -6.7 \times 10^4\,\mathrm{rad\,m^{-2}}$ (Eatough et al. 2013, doi:10.1038/nature12499).
- The RM is far larger than any other sight line through the disc: the Faraday screen must be near the Galactic Centre. Mean $\langle B_\parallel \rangle \gtrsim 1.232\,\mathrm{RM/DM} \approx 46\,\mu\mathrm{G}$ over the whole path; much stronger locally.
- Pulse broadening is far smaller than expected if the screen that broadens Sgr A* sat close to the Galactic Centre: the scattering screen lies well in front of it (Spitler et al. 2014, doi:10.1088/2041-8205/780/1/L3).

Propagation measurements turned a projected position into a physical location.

Assumptions and limitations

- Distances: a single R_0 is assumed for all CMZ structure; true depths differ by $\pm 100\,\mathrm{pc}$ ($\sim 1\%$ in distance, but crucial for association).
- Equipartition fields and energies in NTFs and bubbles are model-dependent.
- Interferometric images filter out smooth emission on large angular scales: absence of extended emission is not evidence of absence.

The rotating neutron star

- $M \approx 1.4\,M_\odot$, $R \approx 10$–$12\,\mathrm{km}$, $I \approx 10^{45}\,\mathrm{g\,cm^2}$ (canonical values).
- Discovered as a periodic radio source (Hewish et al. 1968, doi:10.1038/217709a0).
- Observed: period P and its derivative $\dot{P} > 0$.

Spin-down power (exact for a rigid rotator)

$$\dot{E} = -I\Omega\dot{\Omega} = \frac{4\pi^2 I \dot{P}}{P^3}$$

$\Omega = 2\pi/P$ is the angular rotation rate.
Crab: $\dot{E} \approx 4.5 \times 10^{38}\,\mathrm{erg\,s^{-1}}$ (L15).

Radio luminosity is a tiny fraction ($\lesssim 10^{-4}$) of $\dot{E}$: the radio beam is energetically negligible.

Magnetic dipole braking (cgs)

Assume a dipole of moment $m = B_{\rm s} R^3$ rotating in vacuum, with magnetic inclination $\alpha_{\rm m} = 90^\circ$:

$$\dot{E}_{\rm dip} = \frac{2 m^2 \Omega^4}{3 c^3} \qquad \text{(Larmor formula for a rotating dipole)}$$

Equate to $-I\Omega\dot{\Omega}$:

$$\boxed{B_{\rm s} = \left(\frac{3 c^3 I}{8\pi^2 R^6} P \dot{P}\right)^{1/2} \approx 3.2 \times 10^{19}\,{\rm G}\,(P\dot{P})^{1/2}}$$

- $\dot{\Omega} \propto -\Omega^3$: braking index $n \equiv \Omega\ddot{\Omega}/\dot{\Omega}^2 = 3$. Measured n are mostly < 3: the vacuum dipole is an approximation.
- Integrate with $P_0 \ll P$: characteristic age $\tau_{\rm c} = P/(2\dot{P})$.
- $B_{\rm s}$ and $\tau_{\rm c}$ are model-dependent; only P, $\dot{P}$ (and sometimes $\ddot{P}$) are observed.

Three representative pulsars

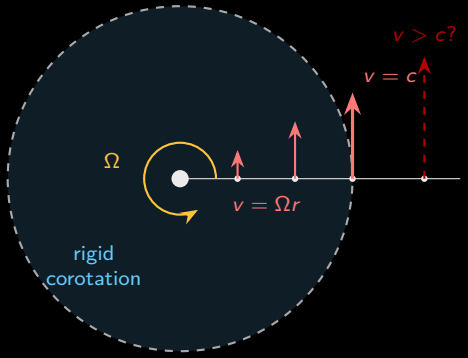
	P	$\dot{P}$	$B_{\rm s}$ (G)	$\tau_{\rm c}$ (yr)	$R_{\rm LC}$ (km)
Crab	33 ms	4.2×10^{-13}	3.8×10^{12}	1.3×10^{3}	1600
Normal (illustrative)	1 s	10^{-15}	1.0×10^{12}	1.6×10^{7}	48 000
MSP (illustrative)	3 ms	10^{-20}	1.7×10^{8}	4.8×10^{9}	140

Three representative pulsars

	P	$\dot{P}$	$B_{\rm s}$ (G)	$\tau_{\rm c}$ (yr)	$R_{\rm LC}$ (km)
Crab	33 ms	4.2×10^{-13}	3.8×10^{12}	1.3×10^{3}	1600
Normal (illustrative)	1 s	10^{-15}	1.0×10^{12}	1.6×10^{7}	48 000
MSP (illustrative)	3 ms	10^{-20}	1.7×10^{8}	4.8×10^{9}	140

- The Crab's true age (SN 1054) is ≈ 970 yr: $\tau_{\rm c}$ is right to within $\sim 30\%$ here, but can be badly wrong when P_0 is not $\ll P$.
- Millisecond pulsars (MSPs): weak fields, ages of Gyr, spun up ("recycled") by accretion from a binary companion. Their rotation is extremely stable: the best clocks.

The light cylinder



View down the rotation axis; arrows show the speed of plasma tied to the star. Not to scale: the star is $\sim 10\,\mathrm{km}$.

Plasma frozen onto the field lines corotates with speed $v = \Omega r$. Set $v = c$:

$$R_{\rm LC} = \frac{c}{\Omega} = \frac{cP}{2\pi}$$

- Inside: field lines close and plasma corotates.
- Outside: corotation would exceed c, so field lines there cannot close: they are open.
- Typical sizes: Crab 1600 km, $P = 1\,\mathrm{s}$ pulsar 48 000 km, MSP 140 km, against $R \approx 10\,\mathrm{km}$.

Summary and further reading

- Galactic Centre: Sgr A West, Sgr A East and Sgr A* overlap on the sky; free-free and H I absorption give the depth order.
- Sgr A* is scatter-broadened as λ^2; the 1.3 mm EHT image works because scattering is small there.
- Filaments and bubbles give only equipartition fields; velocity confusion along $l \approx 0$ means projection is not association.
- A pulsar's RM, DM and scattering turned a projected position into a location (the Galactic Centre magnetar).
- Pulsars: $\dot{E} = 4\pi^2 I \dot{P}/P^3$; $B_{\rm s}$ and $\tau_{\rm c}$ are model-dependent; plasma cannot corotate beyond $R_{\rm LC} = cP/2\pi$.

Further reading

Morris & Serabyn 1996 (Galactic Centre); Heywood et al. 2022 (MeerKAT mosaic); Johnson et al. 2018 (scattering of Sgr A*); Eatough et al. 2013 (magnetar); Lorimer & Kramer 2004, *Handbook of Pulsar Astronomy*; ERA Ch. 6.